Numerical Computation of the Transfer Functions of an Axisymmetric Duct with the Extended Discrete Singular Convolution Method

P.-A. Taillard, T. Hélie and J. Bensoam
IRCAM, 1, place Igor-Stravinsky, 75004 Paris, France
taillard@hispeed.ch

This work takes part of the "cagima" project (supported by the ANR) which investigates the defects of the tuning of reed musical instruments as well as their homogeneity of emission and timbre. The goal consists in replacing the traditional approach adopted by instrument makers by a global and rational approach in the design of new instruments /ab initio/ (called "logical instruments"), minimizing some identified defects. In this context, an interactive virtual model, predictive and configurable is proposed. Several approaches are available in the literature but the main difficulty is to design digital instruments that are accurate (according to measurements) and that can be implemented in real-time. In this paper, an approach based on the Extended Discrete Singular Convolution method (EDSC) is proposed. The temporal operator (including the fractional derivative term for viscothermal losses) is implemented according to the EDSC formalism. The method allows a fast, straightforward and accurate computation of the transfer functions of an axisymmetric duct with an arbitrary profile. The computation of the case where the losses are dependent from the diameter causes no noticeable difficulty. The results are compared to measurements of a trombone bell.

1 Introduction

This work takes part of the "Cagima" project (supported by the French national research agency ANR) which investigates the defects of the tuning of reed musical instruments as well as their homogeneity of emission and timbre. The goal consists in replacing the traditional approach adopted by instrument makers by a global and rational approach in the design of new instruments *ab initio* (called "logical instruments"), minimizing some identified defects. In this context, an interactive virtual model, predictive and configurable has to be developed. Several approaches are available in the literature but the main difficulty is to design digital instruments that are accurate (according to measurements) and that can be implemented in real-time.

The present paper investigates how the Extended Discrete Singular Convolution (EDSC) method [1] can be used for the acoustical simulation of the bore of wind instruments. This method is an extension of the original DSC method proposed by Wei et al. [2], which has proved its efficiency and accuracy for solving differential equations. Technically, this method is based on a "well-suited" family of time-continuous interpolation kernels (delta sequence kernels), which provide the continuous signal from its sampled version. Here, this is used to simulate a 1D model of acoustic propagation in axisymmetric lossy pipes, established in [3] and validated in [4] for straight, conical and flared pipes: the Webster-Lokshin model with curvilinear abscissa (named WL model in the sequel). In this context, the main interest of EDSC (besides accuracy and parsimony) is that the fractional derivative of a signal (operator involved in the model) is derived from the interpolation formula by using the fractional derivative of the kernel, that makes the computation easy. With this method, simulations are performed in the time domain, from which the acoustic transfer functions are deduced in the spectral domain.

This paper is organized as follow: in section 2, the principles of the EDSC method are presented. The section 3 is devoted to the application of this method to the Webster-Lokshin equation. In section 4, a method is given for obtaining numerically the transfer functions from the EDSC simulations. Section 5 is dedicated to the validation of the results with some known analytical results and with measurements of a trombone bell, followed by the conclusions, Section 6.

2 Kernel methods and EDSC

Ideal bandlimited signals $y \in L^2(\mathbb{R})$ (finite energy) with a frequency range included in $[-1/2, 1/2]$ are known to be such that

$$y(t) = \sum_{m\in\mathbb{Z}} y(m)\,\mathrm{sinc}\left(\pi(t-m)\right), \tag{1}$$

where $\mathrm{sinc}(x) = \sin(x)/x$ is the Shannon-Whittaker interpolation kernel [5, 6]. The sampling period is therefore $\Delta t = 1$. This kernel is non causal and with infinite support.

The DSC method has been built in a practical way, so that: (i) an interpolation formula similar to (1) is fulfilled; (ii) the band-limited property is numerically satisfied up to a fixed precision (typically, that of floats); (iii) the kernel magnitude is larger than the fixed precision, on a bounded centered support ($-M \le t \le M$). Such approximations can be recasted in the general framework of Reproducing Kernel Hilbert Spaces [7, cf. p.433] [8], which is not investigated here. The generic formula for the continuous interpolation $\tilde{y}(t)$ of a bandlimited function $y(t)$, its derivatives of order $d > 0$ and its antiderivatives ($d < 0$) is

$$\tilde{y}^{(d)}(t) = \sum_{m=-M}^{M} y(m)\cdot k^{(d)}\left(t-m\right). \tag{2}$$

Different functions can implement the kernel $k(t)$. If $k(t) = \mathrm{sinc}(\pi x)$, $d = 0$ and $M \to \infty$, Eq (1) is retrieved. The kernel has to satisfy (at least up to a fixed precision)

$$\lim_{\alpha\to\infty} \alpha\, k(\alpha t) = \delta(t) \tag{3}$$

where $\delta(t)$ is the Dirac delta distribution. In [2], many kernels are proposed. Among them, an interesting family of symmetrical kernels, efficiently focusing the energy close to $t = 0$, allowing a control of the bandlimited approximation, is defined by the following Regularized Shannon Kernels (labeled RSK in the sequel), for $\sigma > 0$,

$$\mathrm{RSK}(x) = \mathrm{Sinc}(x)\ \mathrm{Exp}(-\frac{x^2}{2\sigma^2}) \tag{4}$$

Note that with $k(t) = \mathrm{RSK}(\pi t)$, $\tilde{y}$ and y coincide at each sample $t = m$ and that, tuning σ and M, their

difference can be made as small as wanted. For a relative level of numerical precision η, the length of the effective numerical kernel support is defined as follows: if $|t| > \ell_k$ then $k(t) < \eta$. Typical value for double precision[1] reals, $\eta \simeq 10^{-15}$, gives rise to $\sigma = 3\pi$ and $\ell_k \simeq 23$.

Because a general expression for $k^{(d)}$ is difficult to find with the RSK kernel, we propose to use another kernel [1]

$$\mathrm{RSK}_N(x) = \frac{1}{2\mathrm{N}} \sum_{n=-\mathrm{N}+\frac{1}{2}}^{\mathrm{N}-\frac{1}{2}} \mathrm{Exp}\left(\frac{inx}{\mathrm{N}} - \frac{x^2}{2\sigma^2}\right) = \frac{\mathrm{RSK}(x)}{\mathrm{sinc}\,(x/(2\mathrm{N}))} \tag{5}$$

with $i = \sqrt{-1}$. Notice that $\mathrm{RSK}_\infty(x) = \mathrm{RSK}(x)$ and, if $k(t) = \mathrm{RSK}_N(\pi t)$, $d = 0$ and $M, N, \sigma \to \infty$, Eq (1) is also retrieved.

This series (5) is rapidly convergent. Moreover it can be shown that a value as small as $N = 15$ builds a kernel which has a numerical accuracy in Eq (2) comparable to that of the RSK kernel (with $\sigma = 3\pi$). In the sequel, the kernel $k(t) = \mathrm{RSK}_N(\pi t)$ with parameters $\sigma = 3\pi$ and $N = 15$ is used, and simply denoted k for sake of conciseness. All numerical examples are computed with this kernel. A general expression for $k^{(d)}$ is given in Appendix A (see also figure 1). For the discrete times

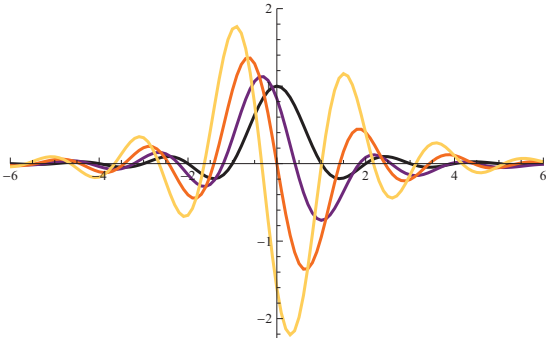

Figure 1: Kernel $k(t) = \mathrm{RSK}_N(\pi t)$ and its derivatives of order $d = \frac{1}{2}$, 1 and $\frac{3}{2}$, according to Eq(13) (from dark to light).

$t = m$, the interpolation formula (2) can be written in vector form as a convolution, $\tilde{\boldsymbol{y}}^{(d)} = \boldsymbol{k}^{(d)} * \boldsymbol{y}$, with $k_j^{(d)} = k(t)^{(d)}|_{t=j}$ and $j = -2M$ to $2M$ by step 1. The vector $\boldsymbol{y}$ has to be padded with M zeros on the left and M zeros on the right, in order to meet the size of the vector $\boldsymbol{k}^{(d)}$. Efficient numerical techniques based on the Fast Fourier Transform can be used to compute this convolution. Doing so, the computing time has approximately linear dependence to M (and not to M^2, as it could be suggested by Eq (2)).

The range $[-M \dots M]$ is called "computing domain". The formula has an optimal accuracy in the "optimal domain" $[-M + \ell_k \dots M - \ell_k]$, whereas in the "truncation domain" $[-M \dots -M + \ell_k,\ M - \ell_k \dots M]$, it may have a poor accuracy, except if $y(m)$ displays small values in this range. This is the main drawback of the method. In the EDSC method, fictitious points are generally implemented in this range [1], in order to perform the most relevant part of the computation in the optimal domain, for instance as

[1] Notice that with $k(t) = \mathrm{sinc}(\pi t)$, a numerical computation up to that precision would be difficult because $\ell_k = 10^{15}$.

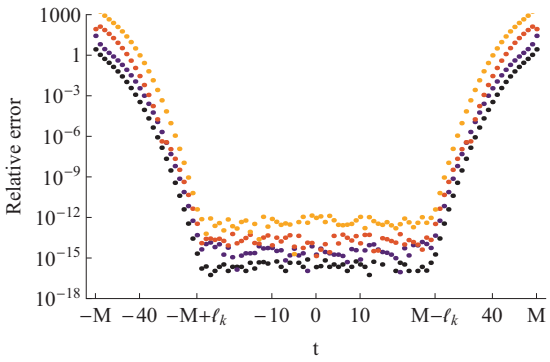

Figure 2: Numerical computation of the derivatives $d = 1, 2, 3, 4$ of a cosine function with Eq (2): Relative error $\left|y^{(d)}(t) - \tilde{y}^{(d)}(t)\right|$, with $y(t) = \cos(t)$ and $M = 50$, comparatively to the exact analytical derivatives $y^{(d)}(t) = \cos(t + d\pi/2)$. From dark to light: derivatives 1 to 4. Length of the effective numerical kernel support: $\ell_k \simeq 23$. The plateau of the "optimal domain" appears clearly.

a polynomial continuation of $y(t)$, which fulfills some boundary conditions, or with the requirement that $y(t)$ is symmetrical or antisymmetrical at the boundaries of the physical problem (located generally at $-M + \ell_k$ and at $M - \ell_k$). These different domains appear clearly in Fig. 2 where the cosine function is chosen as an example (however with $\Delta t = 1/4$, in order to be representative of the accuracy of Eq (2) in the low frequency range).

3 Application to the WL equation

3.1 The Webster-Lokshin equation

The Webster-Lokshin equation (hereafter abreviated WL equation) [4, 9] describes the behavior of the acoustic pressure waves $p(x,t)$ in an 1D axisymmetric duct

$$\left(\partial_x^2 + \frac{2r'(x)}{r(x)}\partial_x\right) p(t,x) = \frac{1}{c^2}\left(\partial_t^2 + 2\epsilon(x)\partial_t^{3/2}\right) p(t,x) \tag{6}$$

and the flow $u(x,t)$, dual quantity to the pressure, is described by the Euler equation

$$-\frac{\rho}{A(x)}\partial_t u(t,x) = \partial_x p(t,x) \tag{7}$$

with parameters $r(x)$: radius of the duct, $A(x) = \pi r^2(x)$: area of the cross section, ρ: density of air, $\epsilon(x) = \kappa_0\sqrt{1 - r'(x)^2}/r(x)$: coefficient of viscothermal losses, and $\kappa_0 \simeq 3.5 \times 10^{-4}$ m$^{1/2}$. The curvilinear abscissa is denoted x in this paper. In order to simplify the discussion, the speed of sound is considered to be $c = 1$.

The analytical solution of this equation for constant $\epsilon(x)$ and constant $\frac{r''(x)}{r(x)}$ is described in [9] and the transfer functions for an arbitrary profile are approximated by concatenation of pieces of pipe with constant curvature and $\mathcal{C}^1$ regularity.

In the present paper we investigate purely numerical solutions of the WL equation for an arbitrary

bandlimited function describing the radius of the duct $r(x)$. A numerical solution can be approximated with the EDSC method. This solution is accurate up to approximately half the Nyquist rate of the temporal mesh.

3.2 Numerical solution with EDSC

We propose an explicit scheme, mixing the ability of the EDSC method for approximating the temporal derivative (including the fractional derivative) and the classical finite differences scheme for the spatial derivative. In order to avoid the problems of accuracy in the "truncated domain" (see Fig. 2), the computing domain must be broad enough to ensure that the acoustic waves have always negligible values in the "truncation domain". A consequence of this choice is that the initial conditions can be specified only for the spatial variable x. This correspond to the physical situation where the pressure and the flow signals are known at a particular coordinate x_0 (or equivalently: where the pressure signals are known at the particular coordinates x_0 and $x_0 - h$, h being a small distance, because flow and pressure are bounded by Eq (7)).

If the signals $p(t, x = x_0)$ and $p(t, x = x_0 - h)$ are bandlimited, Eq (2) permits to approximate the right member of the WL equation (6), at the coordinates $x = x_0$ and $x = x_0 - h$ for all times t (in particular for the discrete times m from $-M$ to M). Let us write these signals in discrete form as a vectors: $\boldsymbol{p}_j = \{p(t = m, x = j)\}$, for all discrete steps m defined above. For any coordinate x, the left member of Eq (6) can be approximated with a classical finite differences centered scheme. This gives rise to the discretization of the WL equation

$$\frac{\boldsymbol{p}_{x-h} - 2\,\boldsymbol{p}_x + \boldsymbol{p}_{x+h}}{h^2} + \frac{r_p(x)\,\left(\boldsymbol{p}_{x+h} - \boldsymbol{p}_{x-h}\right)}{h} \simeq \frac{1}{c^2}\left(\boldsymbol{k}^{(2)} * \boldsymbol{p}_x + 2\epsilon(x)\,\boldsymbol{k}^{(3/2)} * \boldsymbol{p}_x\right) \tag{8}$$

and leads to the explicit scheme for the propagation of the signal in forward direction

$$\boldsymbol{p}_{x+h} \simeq \frac{(h\,r_p(x) - 1)\,\boldsymbol{p}_{x-h} + 2\,\boldsymbol{p}_x + h^2\,\boldsymbol{k}_x * \boldsymbol{p}_x}{h\,r_p(x) + 1} \tag{9}$$

with $r_p(x) = \frac{2r'(x)}{r(x)}$ and $\boldsymbol{k}_x = \frac{1}{c^2}\left(\boldsymbol{k}^{(2)} + 2\epsilon(x)\,\boldsymbol{k}^{(3/2)}\right)$. The spatial progression of the waves in the (infinite) duct can be computed for any arbitrary, bandlimited initial condition $(\boldsymbol{p}_{x_0}, \boldsymbol{p}_{x_0-h})$, by applying the scheme (9) for each spatial step, starting from x_0 and progressing in forward or in backward direction. Since the classical finite differences scheme is much less precise than the EDSC scheme, the spatial step h must be notably smaller than Δt (approximately $h = \Delta t/10$ to $\Delta t/20$), in order to ensure the numerical stability of the scheme[2].

[2]The EDSC scheme has a remarkable, numerical stability, because the RSK kernel damps the high frequency components.

3.3 Practical considerations

In our simulations, the arbitrary initial conditions are defined as a "RSK-impulses":

$$\begin{aligned} p(t, x = 0) &= \mathrm{RSK}(\pi t/\gamma) \\ p(t, x = h) &= \mathrm{RSK}(\pi(t - h)/\gamma) \\ &\text{or} \\ p(t, x = L) &= \mathrm{RSK}(\pi(L - t)/\gamma) \\ p(t, x = L - h) &= \mathrm{RSK}(\pi(L - h - t)/\gamma) \end{aligned}$$

with $\gamma = 1.5$. This choice is motivated by the following considerations: the duration of the RSK-impulse is optimally short (only 70 points are numerically non zero) and it contains all frequencies up to 2/3 of frequency bound of the kernel. The impulse is not centered on zero, because $\boldsymbol{k}_x$ is strongly asymmetrical. On the contrary, the impulse is placed to the leftmost position ensuring that no noticeable numerical reflection occurs on the left boundary. With this placement, the "viscothermal relaxation" due to the "memory" of fractional derivative can be optimally developed.

Despite of this manoeuvre, some numerical reflection occurs on the right boundary, because the "memory" of the 3/2 derivative is very long. This happens even if a temporal mesh of many thousands of points is used, although this makes little sense and wastes computer power only to simulate a sum of decreasing exponentials. The following procedure is more efficient and falsifies the results in a very marginal manner (only on the very low frequency range, where the WL equation has no validity anyway): compute the wave propagation with a quite small value of M (800 or less), cut away the pollution due to the numerical reflection on the right boundary, fit a recursive linear filter according to the "clean" portion of the relaxation "tail" (where the computed signal looks like a decreasing exponential) and extrapolate the decreasing exponential until very small values are reached. In our simulations we used the following recursive linear filter:

$$p(m) = a_1 p(m-n_1) + a_2 p(m-n_2) + a_3 p(m-n_3) + a_4 p(m-n_4) \tag{10}$$

For the trombone bell simulation (see hereafter), the numerical values are: $M = 800$, $n_1 = 1$, $n_2 = 2$, $n_3 = 645$, $n_4 = 1291$. The simulation of the wave propagation was conducted on 20 spatial unities (by steps $h = 1/20$). The RSK-impulse used as initial condition (at $x = 0$ or at $x = L$) was centered 81 points away from the left boundary. The 40 rightmost points of the signal were cut away. The relaxation "tail" was extrapolated up to a total length of 8192 points.

4 Transfer functions

According to the theory of wave guides, the acoustic behavior of a piece of tube of length L (as seen from the input of the piece of tube at $x = 0$ and from the output at $x = L$) can be linked in the frequency domain by a scattering matrix:

$$\begin{pmatrix} U_0 \\ U_L \end{pmatrix} = \begin{pmatrix} H_{11} & H_{12} \\ H_{21} & H_{22} \end{pmatrix} \begin{pmatrix} P_0 \\ P_L \end{pmatrix} \tag{11}$$

When this system of equations is solved for U_0 and U_L (like here), it is named "scattering matrix with

admittance representation". We refer to the functions H_{11}, H_{12}, H_{21} and H_{22} with the generic denomination "transfer functions".

Our concern now is to obtain a discrete numerical version of these transfer functions, computed according to our scheme (9). For this, we have to compute the wave propagation in the piece of tube between $x = 0$ and $x = L$ for 2 different arbitrary initial conditions A and B. The corresponding flows are computed with Eq (7). We notate P_{0A} the Discrete Fourier Transform of the pressure signal $\boldsymbol{p}_0$ for the arbitrary initial condition A, and similarly for P_{0B}, P_{1A} and P_{1B}. The corresponding flows are denoted: U_{0A}, U_{0B}, U_{1A} and U_{1B}. Applying Eq (11) for the arbitrary initial conditions A and B leads to:

$$\begin{aligned} H_{11} &= (-P_{2B}U_{1A} + P_{2A}U_{1B})/C \\ H_{12} &= (P_{1B}U_{1A} - P_{1A}U_{1B})/C \\ H_{21} &= (-P_{2B}U_{2A} + P_{2A}U_{2B})/C \\ H_{22} &= (P_{1B}U_{2A} - P_{1A}U_{2B})/C \\ C &= (P_{1B}P_{2A} - P_{1A}P_{2B}) \end{aligned} \tag{12}$$

5 Validation

5.1 Comparison with the analytic formula

We conducted many simulations for different pieces of pipe with constant curvature and compared the results with the analytical formula given in [9]. The following parameters are used: length of the pipe $L = 70$cm, spatial step $h = 1/20$cm, $M = 400$, extrapolation of the relaxation "tail" on 16384 points. We observed practically no differences in the precision reached by the simulations, between the different curvatures and the different loss coefficients ϵ.

Results: inside the frequency band of validity of the WL equation (about up to 2kHz), the deviation for all transfer functions compared to the analytic formula do not exceed 0.015dB on the module and 0.003rad on the argument. Up to 8kHz, the maximal deviation is: 0.6dB on the module and 0.12rad on the argument.

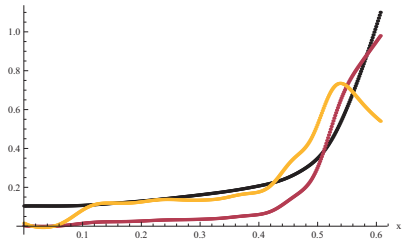

Figure 3: **Bell profil of a trombone**. Abscissa x [in m] and from dark to light: profile of the bell $r(x)$ [in dm], $r'(x)$ and $r'(x)/r(x)$ [arbitrary units].

5.2 Validation with measurements of a trombone bell

The simulation results are compared to the measurements of the input impedance published in [10]

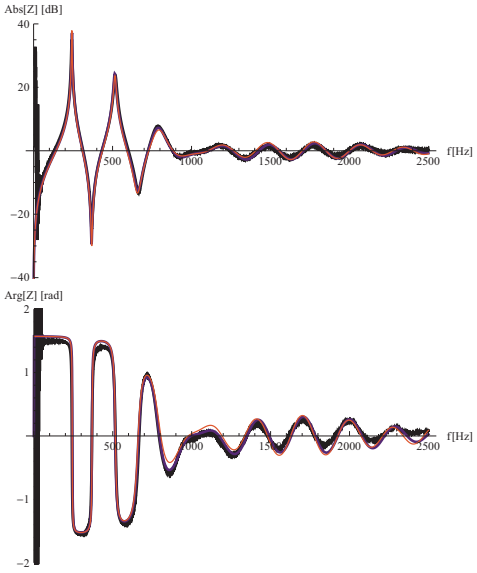

Figure 4: Normalized input impedance of the bell. **Top**: modulus in dB ($20\log_{10}$) **Bottom**: phase in radians. From dark to light: measurement, simulation with the EDSC method and simulation with 5 pieces of pipe with constant curvature, according to [4]

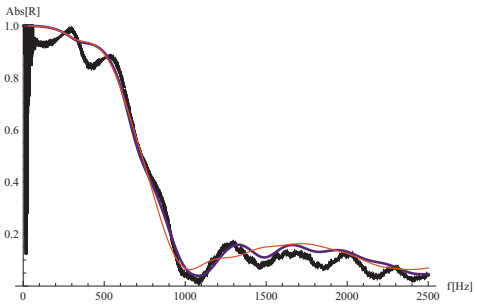

Figure 5: Modulus of the reflection coefficient of the bell. From dark to light: measurement, simulation with the EDSC method and simulation with 5 pieces of pipe with constant curvature, according to [4]

for a trombone bell (Courtois 155R). The curvilinear abscissa x is extracted from the measurements of the radius of the bore (43 points unequally spaced). The radius $r(x)$ and its first derivative $r'(x)$ are interpolated according to Eq (2). The length of the bore is divided in 20 equally spaced steps (plus 5 fictitious points on each side). The corresponding weights $y(m)$ (equally spaced) are obtained by a least squares fit. Fig. 3 illustrates the radius of the trombone bell $r(x)$, its first derivative $r'(x)$ and the ratio $r_p(x) = \frac{2r(x)}{r'(x)}$, plotted along the axis x.

The radiation impedance was simulated according to the model Z_5 used in [4, 11]. The results for the normalized input impedance $Z_{in} = A(0)/(\rho c)P_{in}/U_{in}$ are depicted on Fig. 4. The accuracy is very satisfactory and even better than the best model ($M_\star$) in [4], especially for the phase (between 800 and 1300Hz) and for the reflection coefficient $R_{in} = (Z_{in} - 1)/(Z_{in} + 1)$ (see Fig. 5). We explain this result because the loss coefficient $\epsilon(x)$ varies with the diameter in our model, while in [4], it was taken constant for each piece of pipe constituting the trombone bell.

5.2.1 Computing time

In the context of an interactive design of wind instruments, the recomputing time after a modification of the bore has to be short. We give here some indications of the computing time for the transfer functions of the trombone bell on a quite archaic PC with Intel processor 2.66 GHz. Simulation of 2 propagations with different initial conditions: 0.546 s. Extrapolation of the signals, Fourier Transform and computation of the transfer functions: 0.421 s. Total computing time. 0.967 s.

Computing time of the transfer functions according to [4], as a concatenation of 5 pieces of pipe with constant curvature, according to the analytical formula: 1.186 s. The computing time for the division of the bell into 5 pieces with constant curvature and $\mathcal{C}^1$ regularity is not included.

6 Conclusions

The EDSC method appears to be efficient and accurate for the computation of the transfer functions with the proposed algorithm. The duct has not to be subdivided as usual into different pieces of pipe, which have to be concatenated afterwards. Any bandlimited function can be used in order to define the radius of the duct. The simulation of the wave propagation in the duct requires the computation of one convolution per spatial step. Efficient algorithms are available for this task. The only delicate step is the accurate discretization of $\partial_t^{3/2}\mathrm{RSK}_N(t)$ with the analytical Eq (13), which has to be performed only once and can be stored as a lookup table (see Appendix). The method is promising for solving other equations with fractional derivatives.

Acknowledgments

This work is supported by the French Research National Agency ANR within the CAGIMA project. We also thank the high school ARC-Engineering in Neuchâtel.

References

[1] P.-A. Taillard, B. Gazengel, A. Almeida, and J.-P. Dalmont. Improvements to the discrete singular convolution method and application to beam analysis. *submitted to Journal of Sound and Vibration, available on the HAL server*, 2014.

[2] GW Wei, YB Zhao, and Y Xiang. Discrete singular convolution and its application to the analysis of plates with internal supports. part 1: Theory and algorithm. *International Journal for Numerical Methods in Engineering*, 55(8):913–946, 2002.

[3] Thomas Hélie. Mono dimensional models of the acoustic propagation in axisymmetric waveguides. *J. Acoust. Soc. Amer.*, 114:2633–2647, 2003.

[4] Thomas Hélie, Thomas Hézard, Rémi Mignot, and Denis Matignon. One-dimensional acoustic models of horns and comparison with measurements. *Acta Acustica united with Acustica*, 99(6):960–974, 2013.

[5] John Macnaughten Whittaker. On the cardinal function of interpolation theory. In *Proc. Edinburgh Math. Soc*, volume 1, pages 41–46. Cambridge Univ Press, 1929.

[6] William B Gearhart and HS Schultz. The function sin (x)/ x. *The College Mathematics Journal*, 2:90–99, 1990.

[7] K Yao. Applications of reproducing kernel hilbert spaces–bandlimited signal models. *Information and Control*, 11(4):429–444, 1967.

[8] Nachman Aronszajn. Theory of reproducing kernels. *Transactions of the American mathematical society*, pages 337–404, 1950.

[9] Rémi Mignot, Thomas Hélie, and Denis Matignon. From a model of lossy flared pipes to a general framework for simulation of waveguides. *Acta Acustica united with Acustica*, 97(3):477–491, 2011.

[10] P Eveno, J-P Dalmont, R Caussé, and J Gilbert. Wave propagation and radiation in a horn: Comparisons between models and measurements. *Acta Acustica united with Acustica*, 98(1):158–165, 2012.

[11] Thomas Hélie and Xavier Rodet. Radiation of a pulsating portion of a sphere: Application to horn radiation. *Acta Acustica united with Acustica*, 89(4):565–577, 2003.

A Derivatives of the RSK_N kernel

The RSK_N kernel (5) can be analytically integrated. Moreover, for real values of d (fractional derivatives and antiderivatives), the general expression is

$$\left(\mathrm{RSK}_N(\pi t)\right)^{(d)} = \frac{2^{\frac{d-2}{2}}\pi^{d-\frac{5}{2}}\sigma^{2-d}}{9N}\left(\cos\left(\frac{\pi d}{2}\right)\psi(t,0) + d\sin\left(\frac{\pi d}{2}\right)\psi(t,1)\right) \quad (13)$$

with

$$\psi(t,s) = \Gamma_s \sum_{n=\frac{1}{2}-N}^{N-\frac{1}{2}} e^{-\frac{n^2\sigma^2}{2N^2}}\nu(t)^s\,{}_1F_1\left(\frac{1}{2}(d+s+1), s+\frac{1}{2}, -\nu(t)^2\right)$$

$$\Gamma(t) = \int_0^\infty x^{t-1}e^{-x}\,dx \quad , \quad \Gamma_s = \Gamma\left(\frac{d+1-s}{2}\right)$$

$$\nu(t) = \frac{-Nt - in\sigma^2}{\sqrt{2}N\sigma} \quad , \quad {}_1F_1(a,b,z) = \sum_{k=0}^{\infty}\frac{a_k z^k}{b_k k!}$$

$$a_0 = 1 \quad , \quad a_k = a(a+1)(a+2)...(a+k-1)$$

Notice that the formula (13) is not valid for zero and negative integer values of d, because the Γ function is not defined (analytical formulas for these cases can be found in [1]). The function ${}_1F_1$ is called "Kummer confluent hypergeometric function".